

1 **Identification of novel Bromodomain inhibitors of *Trypanosoma cruzi***
2 **Bromodomain Factor 2 (TcBDF2) using a fluorescence polarization-base**
3 **high-throughput assay**

4 Luis E. Tavernelli^{1,3,◊}, Victoria L. Alonso^{1,2}, Imanol Peña³, Elvio Rodríguez Araya^{1,2}, Romina Manarin²,
5 Juan Cantizani³, Julio Martín^{3,†}, Juan Salamanca³, Paul Bamborough⁴, Felix Calderón³, Raquel Gabarro³,
6 Esteban Serra^{1,2}

7

8 ¹ Instituto de Biología Molecular y Celular de Rosario, CONICET, Rosario, Argentina.

9 ² Facultad de Ciencias Bioquímicas y Farmacéuticas, Universidad Nacional de Rosario, Rosario, Argentina.

10 ³ GlaxoSmithKline Global Health, Tres Cantos, 28760, Madrid, Spain.

11 ⁴ Molecular Design, GlaxoSmithKline, Gunnels Wood Road, Stevenage, Herts, SG1 2NY, UK

12 [†] Current address: Sciengement Lab Consulting, 28750 San Agustin del Guadalix, Spain.

13 [◊] Current address: School of Infection and Immunity. University of Glasgow, Glasgow, Scotland, UK.

14

15 **Abstract**

16 Bromodomains are structural folds present in all eukaryotic cells that bind to other proteins recognizing
17 acetylated lysines. Most proteins with bromodomains are part of nuclear complexes that interact with
18 acetylated histone residues and participate in regulating DNA replication, transcription, and repair
19 through chromatin structure remodeling. Bromodomain inhibitors are small molecules that bind to the
20 hydrophobic pocket of bromodomains, interfering with the interaction with acetylated histones. Using a
21 fluorescent probe, we have developed an assay to select inhibitors of the bromodomain factor 2 of
22 *Trypanosoma cruzi* (TcBDF2) using fluorescence polarization. Initially, a library of 28,251 compounds was
23 screened in an endpoint assay. The top 350 ranked compounds were further analyzed in a
24 dose-response assay. From this analysis, 7 compounds were obtained that had not been previously
25 characterized as bromodomain inhibitors. Although these compounds did not exhibit significative
26 trypanocidal activity, all showed *bona fide* interaction with TcBDF2 with dissociation constants between
27 1 and 3 µM validating these assays to search for bromodomain inhibitors.

28 **Introduction**

29 *Trypanosoma cruzi* is a unicellular parasite that causes Chagas Disease (also known as American
30 trypanosomiasis). It is estimated that at least 6 million people are infected globally, and around 12,000
31 deaths occur annually because of this illness. In the Americas, Chagas disease is the most important
32 parasitic disease, with an annual incidence of 30,000 new cases on average, among them 8,600 are
33 newborns that become infected during pregnancy ¹. Originally, Chagas disease was constrained within
34 Latin American countries, but recent emigration movements have spread the infection to other
35 territories such as Spain, the USA, or Canada ². Only two active compounds are currently being used to

36 treat the disease: Nifurtimox and Benznidazole, both developed more than fifty years ago. These
37 compounds display severe side effects and even though their use in the acute phase of the disease is
38 efficient, their use in the chronic phase is still controversial ³. These facts highlight the need for new,
39 improved, and efficient drugs against this deadly disease.

40 Lysine acetylation is a reversible post-translational modification (PTM) found in a myriad of proteins, but
41 the exact function of this PTM is just starting to be understood. In the past years, the target proteins
42 that were subjected to this modification were found to be involved in distinct nuclear processes such as
43 transcription, DNA replication, and repair, presumably due to chromatin remodeling ⁴. Nowadays,
44 acetylation is known to be present in all cellular compartments participating in diverse processes like
45 energetic metabolism, protein degradation, protein localization, and cell cycle regulation, among others
46 ^{5,6}.

47 Bromodomains (BD) are ~110 amino acid-long protein modules that specifically recognize and bind to
48 acetylated lysines (AcK). These domains bear a left-handed four- α -helix bundle structure (α A, α B, α C,
49 and α Z) connected by two loops (ZA and BZ loops) that form the accessible hydrophobic pocket where
50 the recognition of the Ac-K takes place ⁷. Currently, it is known that there are eight coding sequences for
51 BD-containing proteins in trypanosomatids, named *TcBDF1* to *TcBDF8* ^{8,9}. Our lab has been pioneering in
52 the characterization of BDs in *T. cruzi* throughout the years ^{10–14}. The first bromodomain to be studied in
53 our group was *TcBDF2*, which is expressed throughout the parasite's life cycle and is found in discrete
54 regions within the nucleus ^{12,14}. Furthermore, this protein bears a bipartite Nuclear Localization
55 Sequence (NLS) that targets the bromodomain in the nucleus. Also, *TcBDF2* was shown to be important
56 in the development of infection *in vitro* as well as the kinetics of the replicative stages in epimastigotes.
57 We have shown that this bromodomain can interact with histone H2 and H4 (through the acetylated
58 lysines 10 and 14). In addition, a recent study demonstrated that *TcBDF2* was associated with H2B.V and
59 directly interacts with the histones H2B.V, H2B, and H4 in *in vitro* assays ¹⁵.

60 Out of a limited number of cases with cytoplasmic or dual localization ^{10,11,16–18}, BDs compose a family
61 of proteins that are usually known as "readers" that recognize acetylation marks on histones. Once the
62 "reading" takes place, bromodomains act as bridges or scaffolds for the assembly and/or recruitment of
63 other factors allowing the interaction with the chromatin within that region ¹⁹. BD-driven recruitment of
64 complexes into the chromatin influences key regulatory processes within the nucleus such as
65 transcription, DNA repair, and DNA replication, among others. All these processes must be carried out in
66 a precise and regulated manner, where an unbalanced regulation or incorrect function of BD factors can
67 be associated with cell death or uncontrolled proliferation. For example, in many types of cancers or
68 chronic inflammatory diseases, BD factors are upregulated and considered potential targets for new
69 drug discovery campaigns ²⁰.

70 The development and discovery of small molecules that can bind and inhibit proteins is a rapidly
71 advancing field of research. In the past years, many molecules against bromodomains have been
72 identified, proving their efficacy as active inhibitors. To date, according to the Clinical Trials Database
73 from the National Academy of Medicine, there are 55 studies (either completed or still running) with BD
74 inhibitors mainly targeted to different types of cancer and inflammatory diseases, among others
75 (<https://clinicaltrials.gov/>, last consultation 12/12/23). In this context, parasitic bromodomains have also

76 been gaining attention as attractive targets to battle NTDs such as American trypanosomiasis,
77 Leishmaniasis, Malaria, and Toxoplasmosis²¹⁻²⁷.

78 In a previous report, we established the relevance of *TcBDF2* in all the stages of the parasite and
79 described a small set of molecules, already known as mammalian BD inhibitors that were able to bind
80 specifically to *TcBDF2*¹⁴. In the present study, we describe a high-throughput competition assay based
81 on Fluorescent Polarization (FP) that allowed us to identify molecules that bind to *TcBDF2*. After this
82 initial screening, the binding of the selected compounds was confirmed by Thermal shift and the
83 cytotoxicity was tested against different life cycle stages of *T. cruzi*. We were able to identify *TcBDF2*
84 inhibitors that serve as a starting point for rationally designing new compounds to be explored against
85 Chagas disease.

86

87 **Material and Methods**

88 **Protein Purification**

89 *Escherichia coli* BL21 carrying pDEST17-*TcBD2* and pDEST17-*TcBD2m* (mutant BD2: Y85A and W92A
90 without the ability to bind to acetylated Histone 4²⁸) were grown at OD ~ 0,6 and induced with 0.1 mM
91 isopropyl-β-D-thiogalactopyranoside during 4 hours at 37°C as described previously¹⁴. The proteins
92 were purified using Ni-NTA (Thermo FisherTM) following the manufacturer's instructions. The purified
93 proteins were dialyzed against the previously determined optimal assay buffer: phosphate 0.1 M pH=8,
94 glycerol 1%, DMSO 0.5%, and diluted to a final concentration of 200 μM. Correct secondary structure of
95 soluble proteins was verified by circular dichroism spectroscopy using a spectropolarimeter (Jasco J-810,
96 Easton, MD, USA).

97 **Fluorescence polarization (FP) assay setup and data analysis**

98 FP measurement was performed on a BMG PheraStar FS plate reader (BMG Labtech GmbH, Ortenberg,
99 Germany) at an excitation wavelength of 488 nm and an emission wavelength of 675 nm (50 nm
100 bandwidth) and Black 1536-well flat bottom small volume microplates with a non-binding surface from
101 Greiner Bio-One GmbH (Frickenhausen, Germany). Optimal Bromosporine (BSP) probe/*TcBD2*
102 interaction conditions were assayed by including in the reaction phosphate medium and seriated
103 dilutions of DMSO (up to 2%), DTT (up to 50 μg/ml), EDTA (up to 90 μg/ml), glycerol (up to 10%), BSA (up
104 to 250 μg/ml), deoxy big-chaps (up to 50 μg/ml), CHAPS (up to 50 μg/ml), Zwittergent 3-14 (up to 50
105 μg/ml), Triton-X100 (up to 0,5 M), NP40 (up to 0.3 M), Tween-20 (up to 100 μg/ml) and Pluronic acid (up
106 to 10%). The final conditions of the screening assay were set at a final volume of 8 μl, 50 nM of the
107 Bromosporine probe (BSP-AF488), and 100 μM of *TcBDF2*, phosphate pH=8, glycerol 1 %, and DMSO 0.5
108 %. Recombinant *TcBD2m* was used as a negative control of binding. For the screening, 8 microliters of
109 recombinant *TcBD2* contained in the assay buffer plus 50 nM of BSP-AF488 were dispensed in 1,536
110 wells Grenier plates were compounds resuspended in 8 μL of DMSO, were previously dispensed. The
111 primary screening was performed at a single shot at a final concentration of 100 μM per well. Further
112 on, to determine the compounds' potency 11-concentration points in a 1:3 seriated dilutions pattern
113 were stamped in the plate, starting at 100 μM. Plates were stored frozen at -20°C until used when they
114 were allowed to equilibrate at room temperature before proceeding to the reading. Controls were made

115 by using recombinant *TcBD2m* instead of *TcBD2*, under the same conditions. All manipulations were
116 made by using Multidrop™ Combi Reagent Dispenser.

117 Statistics, Z values, and robustness (3SD) to determine activate cutoff were calculated using templates in
118 ActivityBase.

119

$$\text{Inhibition (\%)} = \left(\frac{mP_{\text{positive control}} - mP_{\text{compound}}}{mP_{\text{positive control}} - mP_{\text{negative control}}} \right) \times 100$$

120

121 The validation of the assay performance for each enzyme was quantified by calculation of the Z'-factor
122 using the formula:

$$Z' = \left| \frac{3\sigma_+ + 3\sigma_-}{\mu_+ - \mu_-} \right|$$

123

124 where σ_+ and σ_- are the standard deviations and μ_+ and μ_- are the mean values of the positive and
125 negative controls, respectively. A series of negative and positive controls was measured. For each,
126 positive and negative control, 64 wells were analyzed.

127

128 Thermal shift

129 Recombinant *TcBD2* was buffered in 10 mM HEPES, pH 7.5, and 300 mM NaCl and assayed in a 96-well
130 plate at a final concentration of 5 μ M in a 25 μ L volume. Compounds were added at a final
131 concentration between 1 and 50 μ M to calculate dissociation constants. SYPRO Orange was added as a
132 fluorescence probe at a dilution of 1:10000. Excitation and emission filters for the SYPRO Orange dye
133 were set to 465 and 590 nm, respectively. The temperature was raised with a step of 2°C per minute
134 from 25°C to 96 °C, and fluorescence readings were taken at each interval in a real-time Biorad Opus
135 CFX. Data were analyzed as previously described ²⁹.

136

137 Molecular Modeling

138 **Protein preparation and grid generation for docking:** The crystal structure of *TcBDF2* solved with
139 bromosporine (PDB entry 6NIM, resolution = 1.78 Å) was used as a reference structure for modeling in
140 Maestro (Schrodinger Release 2022-2: Maestro Schrodinger LLC: New York, 2022) ³⁰. The selection of the
141 structure was based on the occupation of the bromosporine at the active site and the good resolution.
142 The Protein Preparation Wizard module was used to remove solvent molecules, add missing side chains
143 (Thr9, Lys27, Lys45, Lys64, Lys88 placed outside of the binding pocket), add hydrogens (PROPKA pH 7.0),
144 and minimize the structure under the OPLS4 force field with heavy atoms restrained to 0.3 Å RMSD.
145 Additionally, four buried water molecules (W 304, 305, 316, 327 according to the residue number of PDB
146 6NIM; see SI) were retained at the bottom of the binding cavity 42-43. The grid was defined as a closed
147 box centered at the bromosporine, and other settings were set to default values.

148 **Ligand preparation for docking:** Chemical structures (compounds) were prepared using LigPrep to
149 generate the 3D conformations. The protonation states were generated at pH 7.4 \pm 0.5 and geometry
150 optimization with the S-OPLS force-field.

151 **Docking protocol:** Docking was performed using Maestro with the extra precision (XP) mode using Glide.
152 Ligand sampling was set to flexible and Epik state penalties to docking score were included. The

153 hydrogen bonds with Asn86 and Trp304 were selected as constraints where at least one of them must
154 match.

155

156 **Beta-galactosidase expressing parasites assay**

157 *T. cruzi* Dm28c which expresses the *Escherichia coli* LacZ gene was used ³¹⁻³³. Epimastigotes were
158 incubated with the compounds (50, 25, 12.5, 6.25 and 3.125 μ M). After 72 h of treatment the assays
159 were developed by the addition of Chlorophenol red- β -D-galactopyranoside (CPRG) (100 μ M final
160 concentration) and Nonidet P-40 (0.1% final concentration). Plates were incubated for 2 to 4 hours at
161 37°C. Wells with β -galactosidase activity turned the media from yellow to red, and this was quantitated
162 by Absorbance at 595 nm using a Synergy HTX multi-detection microplate reader as reported previously
163 ³¹. Normalized survival percentage was plotted against concentrations on Prism 9.0 GraphPad software.
164 DMSO 50% was used as the zero percent survival baseline. Each concentration was assayed in
165 triplicates.

166

167 **MTT Assay**

168 Cell viability after treatment was determined by the 3-(4,5-dimethylthiazol-2-yl)-2,5-diphenyltetrazolium
169 bromide (MTT) reduction assay as previously described ²⁹. Briefly, Vero cells (5.000 cells per well) were
170 incubated in a 96-well plate in the presence of each compound (200, 100, 50, 25 and 12.5 μ M) for 48
171 hours. Then 200 μ L MTT solution (5 μ g mL-1 in PBS) was added to each well and incubated for 1 hour at
172 37°C. After this incubation period, the MTT solution was removed and precipitated formazan was
173 solubilized in 100 μ L of DMSO. Optical density (OD) was spectrophotometrically quantified (λ = 540 nm)
174 using a Synergy HT multi-detection microplate reader. DMSO was used as blank, and each treatment
175 was performed in triplicates. IC₅₀ values were obtained using non-linear regression on Prism 9.0
176 GraphPad software.

177

178 **Results and discussion**

179 **Identification of *TcBD2* binders through a fluorescence polarization-based high throughput 180 screening**

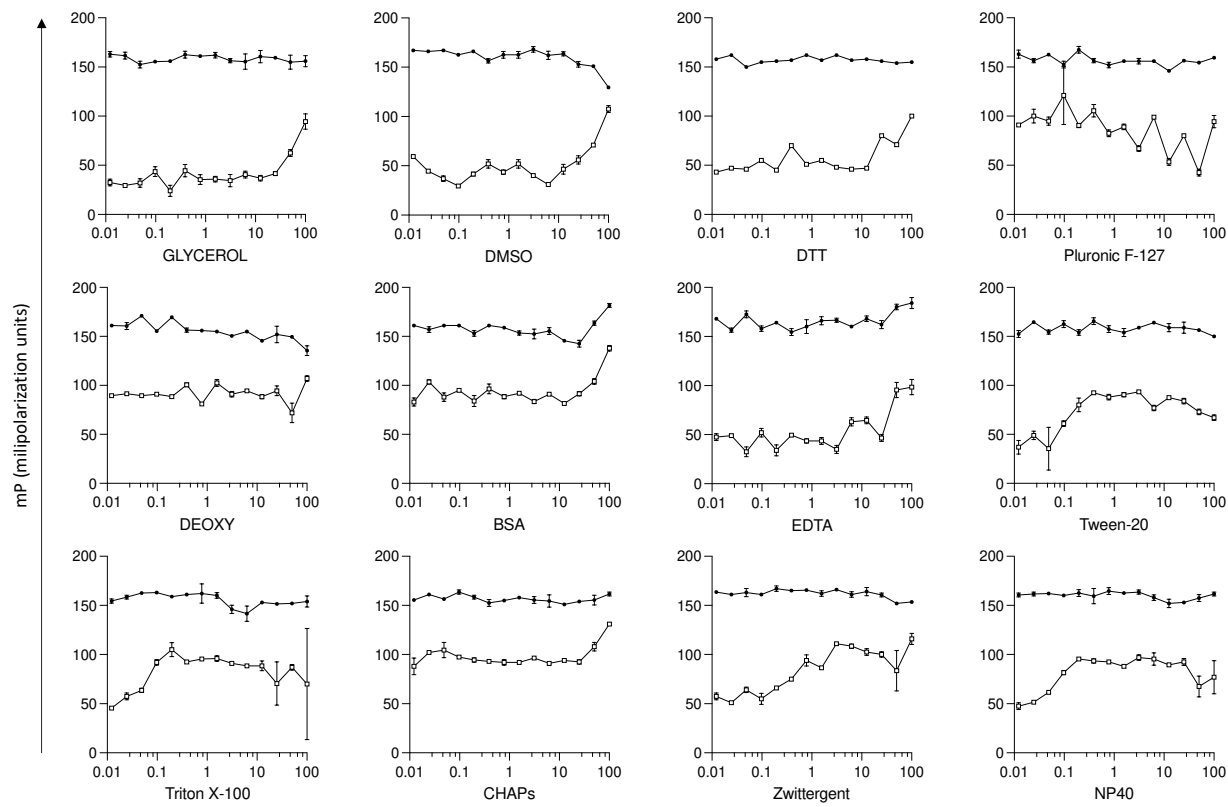
181 To identify molecules that bind to the *TcBDF2* bromodomain (*TcBD2*), we set up a high-throughput
182 screening (HTS) assay using Fluorescent Polarization (FP). FP is a very sensitive technique that allows
183 quantitative analysis of the interaction between two molecules. Recent developments have allowed this
184 technique to be adapted to be used in HTS format toward finding inhibitors against a myriad of proteins
185 ^{34,35}.

186 Firstly, we assayed previously used fluorescent probes with an affinity for the mammalian BDs ATAD2³⁶,
187 PCAF and GCN5³⁷, BRPFs³⁸, Brd9 that is also a promiscuous human Brd binder³⁹, BET BD1 selective⁴⁰ and
188 BET BD2 selective (Patent WO2014140076). None of these probes showed significant fluorescence
189 polarization when incubated with recombinant *TcBD2* under standard conditions, reinforcing the idea
190 that these parasite BDs are very divergent from human ones.

191 Given that we previously showed that the BD-pan inhibitor Bromosporine (BSP) binds to *TcBD2* ¹⁴, we
192 decided to modify this molecule to use it as a fluorescent probe in the HTS assay. Hence, AlexaFluor-488

193 (AF488) was coupled to BSP (Fig. S1). BSP was our last choice because we have previously demonstrated
194 that it has no significative trypanocidal activity¹³. BSP-AF488 probe was used with the wild-type (*TcBD2*)
195 and a previously characterized recombinant mutant version of *TcBD2* (*TcBD2m*, unable to bind to its
196 acetylated ligand) to optimize the conditions in a HTS format. We first tested different buffer
197 compositions to obtain a working window of approximately 120 mP, needed to proceed to the screening
198 assay. Optimal conditions for the screening were determined as shown in Figure 1. Screenings were
199 made in a 1,536 plate with a final volume of 8 μ L. The condition selected was: 100 μ M of recombinant
200 *TcBD2*, 50 mM of BSP-AF488, buffer phosphate 0.1 M, glycerol 1 %, and DMSO 0.5 %. Recombinant
201 *TcBD2m* was used as a negative control in all plates assayed. As can be observed, there is very low
202 interaction between the probe and BD2m in all conditions tested. The Z' score, calculated as mentioned
203 in the Methods section, was used as a quality control parameter⁴¹.

204



205

206

207 **Figure 1: Fluorescent polarization assay setup.**

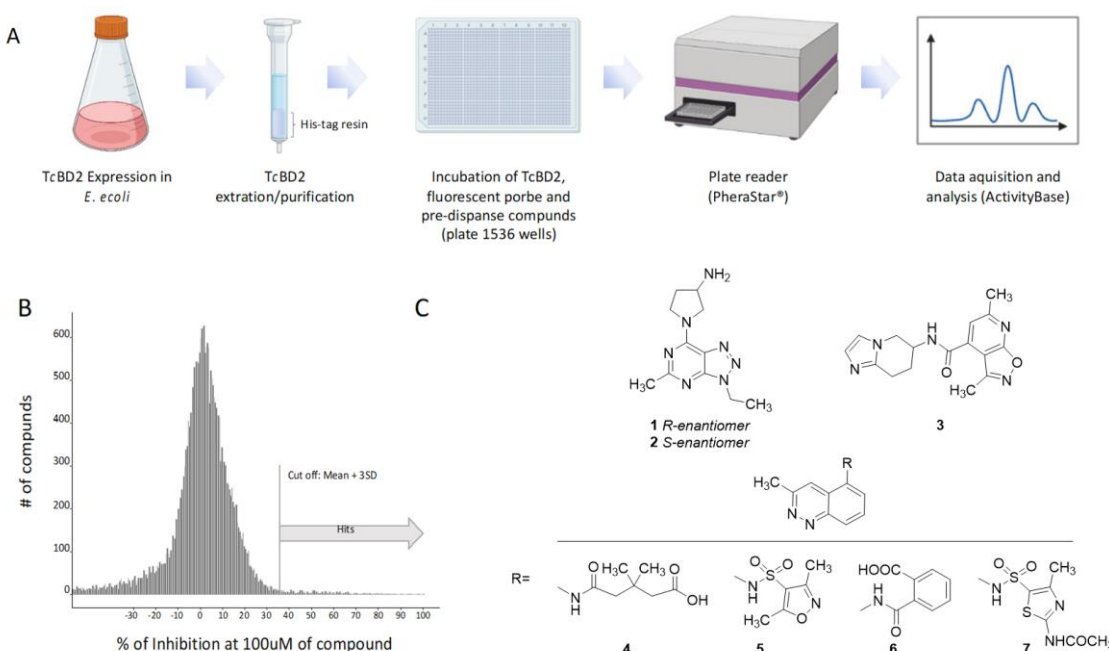
208 Different additives to the buffer used for the assay were tested to find the best conditions. All indicated reagents
209 (below the graphs) were assayed in a 50 mM phosphate buffer pH=8. Concentrations assayed are indicated in the
210 Methods section and were normalized in a logarithmic scale on the X-axis. On the y-axis polarization fluorescence
211 is indicated in mP units. Recombinant *TcBD2m* was used as a negative control of binding. Grainer plates of 1536
212 wells were used for all assays and the reading was made with PheraStar Technology. (○)TcBD2m, TcBD2WT (●).

213

214 Once the assay conditions were established, we performed the screening of a small molecule
215 bromodomain-targeted compound set (summarized in Fig. 2A). The set mostly consisted of compounds

216 showing experimental activity against bromodomains or synthesized during various human
217 bromodomain drug discovery programs, and their analogs (total of 28,251 compounds). The library was
218 tested in a single shot format at a final concentration of 100 μ M, in a 1,536-wells plate format. All plates
219 assayed were analyzed using in-house algorithms and the Z' score (over 0.4) was used as a quality
220 control parameter.
221 Out of all compounds tested, 471 compounds were considered positive after the first single shot format
222 assay was performed. The cut-off for positive hits was set at (mean + 3SD) or 37% inhibition, having a
223 positive hit rate of 1.7% (Fig. 2B). Next, to determine the compounds' potency, 11 concentration points
224 in a 1:3 dilution pattern were stamped in a 1,536-plate starting at 100 μ M. Recombinant *TcBD2m* was
225 used as a negative control. In this assay, 7 compounds showed binding activity of $\text{pIC50} \geq 4,5$ against
226 *TcBD2* in a dose-response manner (Fig. 2C, Table 1).

227



228

229 **Figure 2: HTS assay to identify *TcBD2* binders.**

230 A) Schematic flowchart of HTS assay. B) Histogram representing 28,251 compounds assayed in a single shot format
231 using 1,538 grainer plates. All compounds were tested at a final concentration of 100 mM. The cut-off to consider
232 positive hits was set at 37% of inhibition. *TcBD2* was used as positive (100% fluorescent probe bound to the BD)
233 and *TcBD2m* as negative (100% fluorescent probe non-bound to BD). Z' score was used as the quality control
234 parameter where only plates with Z' score of above 0.4 were considered for analysis. C) Structures of hits with
235 $\text{pIC50} \geq 4,5$ resulting from the seriated dilutions screening of the 350 selected compounds (all compounds were
236 >90% purity). Figure 2A was created with Biorender.com.

237 The binding of the 7 selected compounds to *TcBD2* was verified by differential scanning fluorimetry
238 (DSF) or Thermal shift observing K_{ds} between 1 and 3 μ M (Table 1 and Fig. S2). The (most promising)
239 compounds were modeled at the AcK site of *TcBD2* to further validate their potential role as inhibitors
240 (Fig. S46). Importantly, AcK binds in a heavily hydrophobic pocket but contains several well-resolved

241 structural waters in the binding pocket. These water molecules are observed at the base of the pocket in
242 most BRD as well as in the X-ray structure of *TcBDF2* (Fig S3)^{42,43}. AcK recognition is mediated by a direct
243 hydrogen bond to a conserved asparagine (Asn 86 in *TcBDF2*), which is mimicked by most BRD inhibitors.
244 Moreover, there is also a conserved tyrosine (Tyr43 in *TcBDF2*) to coordinate the active site bridging
245 water molecule⁴⁴ (Fig. S3). Both interactions are also conserved in the crystal structure of *TcBDF2* with
246 BSP. We evaluated whether the compounds were able to retrieve those interactions at the AcK pocket
247 through molecular modeling (while binding to the AcK pocket). The docking procedure was validated by
248 reproducing the binding mode of bromosporine while maintaining key interactions (Fig. S4). Docking
249 studies revealed that all seven compounds fit into the substrate pocket of *TcBDF2*. The compounds were
250 able to form a hydrogen bond with Asn86 and/or the water-bridged hydrogen bond with Tyr43 (Fig.
251 S5-S6). It is worth mentioning that compounds 4, 5, 6, and 7 with methylcinnoline as core made
252 pi-stacking interaction with Trp92, and even 4 and 5 can form a hydrogen bond in a similar way to BSP
253 (Fig. S5-6). The docking pose of compound 3 placed the dimethyl-isoxazole-pyridine moiety rotated 180°
254 vertically from the expected position, as is the case with the AcK mimic methylbenzoisoxazole (PDBid
255 5Y8C)⁴⁵. The enantiomer compounds 1 and 2 also made a pi-cation interaction with Trp92, where they
256 can also form pi-stacking interactions between the 3-ethyl-5-methyl-triazolopyrimidine core and Trp92
257 (Fig. S6).

258 **Table 1. Dissociation constants and binding measured by thermal shift over recombinant *TcBD2*.**

Compound	1	2	3	4	5	6	7
<i>pKd</i>	5.8	1.9	5.6	5.8	3.52	5.4	5.5
<i>pIC50</i>	4.6	4.5	4.7	5.1	5.6	4.5	4.8

259

260 Finally, the 7 compounds were tested in an *in vitro* assay of *T. cruzi* intracellular amastigote assay using
261 VERO cells as hosts⁴⁶ and in an *in-house* colorimetric assay using epimastigotes of the Dm28c strain that
262 expresses beta-galactosidase from an episomal plasmid (Fig. S7)³¹. Not surprisingly, none of the
263 compounds showed parasiticidal activity at concentrations below 50 μM in the two life cycle stages.
264 Additionally, we assessed the toxicity of these compounds in the cell line used for the infection assays
265 using MTT. Our results indicate that none of the compounds exhibited cytotoxicity up to 200 μM (data
266 not shown).

267 **Conclusions**

268 We have previously assayed the binding of *TcBDF2* and *TcBDF3* to several BD inhibitors and determined
269 that they have different binding specificities^{13,14}. Commercial human inhibitors iBET-151 and BSP bind to
270 both bromodomains; but JQ1(+), which binds *TcBDF3* with an affinity similar to iBET-151, does not
271 interact with *TcBDF2*. The compounds from the HTS we tested herein have *Kds* for *TcBD2* between 1 and
272 3 μM, however, they have no significative activity against epimastigotes, nor amastigotes in infected
273 cells. This effect could be due, at least in part, to a low potency of the compounds obtained in our
274 screening, a fact that could be associated with the use of BSP as a probe, a compound that, itself, shows
275 low trypanocidal activity. Also, a possible explanation for this lack of activity of *TcBDF2* inhibitors could
276 be associated with the multimeric nature of the complexes in which bromodomains are included (see
277 below).

278 The human inhibitors mentioned were also assayed against BDF orthologues from other
279 trypanosomatids with different results. Schulz and coworkers showed that iBET-151 (BET bromodomains
280 inhibitor) induces *T. brucei* bloodstream form to develop insect-stage features, like the expression of
281 surface procyclin and upregulation of glycolysis enzymes. They found that *TbBDF2* and *TbBDF3* bind
282 iBET-151 with a low affinity ($K_d=225 \mu M$ and $175 \mu M$, respectively) and do not bind at all to other BET
283 inhibitors like JQ1(+). iBET-151 was co-crystallized with *TbBDF2*, and it was found in a completely atypical
284 position, flipped by roughly 180° to the position it binds to human BDs, something that could explain the
285 low affinity of the interaction ^{21,47}. Later, Yang and collaborators assessed 27 compounds obtained by a
286 structure-based virtual screening combined with ITC experiments. They found one compound (GSK2801)
287 that binds with higher affinity to the BD of *TbBDF2* ($K_d=15 \mu M$) and with lower affinity to the second BD
288 of *TbBDF5* ($K_d=83 \mu M$). By contrast, GSK2801 does not bind to *TbBDF3* or the first BD from *TbBDF5* ⁴⁸.
289 *BDF5* from *Leishmania donovani* was also recently assayed against human BD inhibitors ²⁷. *LdBDF5* binds
290 to SGC-CBP30, BSP, and I-BRD9, with different affinities for the first or second DB. SGC-CBP30, which
291 showed the higher affinity ($K_d=281 nM$, for *LdBDF5.1*), also exhibited activity against promastigotes from
292 *L. mexicana* ($IC_{50}=7,16 \mu M$) and *L. donovani* ($IC_{50}=6,16 \mu M$).

293 It is worth mentioning that not always a direct correlation is found between the affinity of the inhibitors
294 and their activity against the parasite in *T. cruzi* nor *T. brucei* or *Leishmania*. For example, iBET-151 and
295 JQ1(+) have IC_{50} against Dm28c epimastigotes of $6.35 \mu M$ and $7.14 \mu M$ respectively ¹³. In contrast, BSP
296 that has a K_d for *TcBDF2* similar to iBET-151 was less active against parasites ($IC_{50} > 50 \mu M$). GSK2801
297 inhibits the growth of procyclic *T. brucei*, disrupting the nucleolar localization of *TbBDF2*, with an IC_{50} of
298 $1.37 \mu M$, which suggests that GSK2801 has other targets beyond the inhibition of *TbBDF2* ⁴⁸. Also, as was
299 mentioned above, the IC_{50} for SGC-CBP30 against *Leishmania* promastigotes was significantly lower than
300 the K_d measured for this compound on *LdBDF5.1*.

301 Staneva and coworkers established that the majority of *T. brucei* BDFs participate in complexes that
302 include other BDFs ⁴⁹. A similar situation was reported by Jones and coworkers for *LdBDF5* ⁵⁰. In this
303 situation, which seems to be characteristic of trypanosomatids, limited inhibition of only one BD of the
304 complex could be countered by the presence of another one or ones. However, over-expression of
305 dominant negative mutants of one of the BDFs would induce disruption of the whole complex and a
306 more deleterious effect over the parasite, as we have previously reported for *TcBDF2* ²⁸. This model
307 could also explain the results obtained for other BD inhibitors in other trypanosomatids. Moreover,
308 extrapolating when determining the essentiality of BDFs in these parasites should be made with caution.

309 The activity of bromodomain inhibitors was also determined for other parasites showing intriguing
310 results. Chua and coworkers assayed 42 compounds previously characterized as BD inhibitors for activity
311 against the asexual form of *Plasmodium falciparum*. All compounds were predicted to be correctly
312 placed into the BD of *P. falciparum* histone acetyltransferase *PfGCN5* and to interact with the conserved
313 asparagine by a hydrogen bond, but these interactions were not experimentally measured. SGC-CBP30,
314 a selective inhibitor of human CREBBP (CBP) and EP300 bromodomains, showed the highest *in vitro*
315 activity, with an IC_{50} of $3.2 \mu M$ and a selectivity index (calculated using a human HEK 293 cell line) of
316 around 7 ²⁴. Finally, *Toxoplasma gondii* was assayed with L-Moses, a specific inhibitor for the
317 GCN5-family bromodomains ²⁶. L-Moses interferes with the *in vitro* interaction of GCN5b bromodomain

318 with acetylated histone residues and displays potent activity against *Toxoplasma* tachyzoites infecting
319 HFF cells (IC₅₀ of ~0.6 μM).

320 All this evidence suggests that maybe targeting only one BD is not the best strategy against
321 trypanosomatids. An alternative could be designing pan-inhibitors against BDs present in nuclear protein
322 complexes taking advantage of the divergence in parasitic BDs vs. human BDs. However, it is hard to
323 conceive that such kind of compound could be designed. Another alternative could be focusing on BDs
324 with novel localizations outside the nucleus that are druggable, at least in *T. cruzi*, and do not take part
325 in protein complexes with other BDs ^{29,51}.

326 In summary, we identified 7 hits competitive against *TcBDF2* in a fluorescence polarization assay and
327 validated their binding by DSF. The confirmed hits originated from a set of compounds targeting human
328 bromodomains, but despite bearing some features reminiscent of previously published bromodomain
329 inhibitors they are structurally distinct. Except compound 3, all have been tested in various historical
330 hBRD4 assays at GlaxoSmithKline and did not give fitted BRD4 dose-response curves at concentrations
331 up to 50 μM. We are therefore confident that the hits are not generally promiscuous bromodomain
332 inhibitors but may represent specific binders to *TcBDF2* with some selectivity over the BET family, the
333 most studied human bromodomain-containing proteins and those whose potential clinical safety risks
334 are best understood. While these hits bind more weakly to *TcBDF2* than clinical inhibitors of human BET
335 bind to their targets *in vitro* (typically at least 100 nM), they represent good starting points for
336 optimization.

337 **Acknowledgments**

338 This work was supported by Tres Cantos Open Lab Foundation (Tc261) and Agencia Nacional de Ciencia
339 y Tecnología from Argentina (PICT-2017-1978, PICT-2020-SERIEA-01704) and Universidad Nacional de
340 Rosario (1BIO490). We would like to thank Dolores Campos for their technical assistance with Vero cell
341 and parasite culture.

342 **Bibliography**

- 343 (1) *Chagas disease - PAHO/WHO / Pan American Health Organization*.
344 <https://www.paho.org/en/topics/chagas-disease> (accessed 2023-06-13).
- 345 (2) WHO. *WHO / Chagas disease (American trypanosomiasis) Factsheet*. WHO.
- 346 (3) Malone, C. J.; Nevis, I.; Fernández, E.; Sanchez, A. A Rapid Review on the Efficacy and Safety of
347 Pharmacological Treatments for Chagas Disease. *Trop Med Infect Dis* **2021**, *6* (3).
348 <https://doi.org/10.3390/tropicalmed6030128>.
- 349 (4) Chen, Y. J. C.; Koutelou, E.; Dent, S. Y. R. Now Open: Evolving Insights to the Roles of Lysine
350 Acetylation in Chromatin Organization and Function. *Mol Cell* **2022**, *82* (4), 716–727.
351 <https://doi.org/10.1016/J.MOLCEL.2021.12.004>.

352 (5) Ali, I.; Conrad, R. J.; Verdin, E.; Ott, M. Lysine Acetylation Goes Global: From Epigenetics to
353 Metabolism and Therapeutics. *Chem Rev* **2018**, *118* (3), 1216.
354 <https://doi.org/10.1021/ACS.CHEMREV.7B00181>.

355 (6) Shvedunova, M.; Akhtar, A. Modulation of Cellular Processes by Histone and Non-Histone Protein
356 Acetylation. *Nat Rev Mol Cell Biol* **2022**, *23* (5), 329–349.
357 <https://doi.org/10.1038/S41580-021-00441-Y>.

358 (7) Zeng, L.; Zhou, M. M. Bromodomain: An Acetyl-Lysine Binding Domain. *FEBS Lett* **2002**, *513* (1),
359 124–128. [https://doi.org/10.1016/s0014-5793\(01\)03309-9](https://doi.org/10.1016/s0014-5793(01)03309-9).

360 (8) Aslett, M.; Aurrecoechea, C.; Berriman, M.; Brestelli, J.; Brunk, B. P.; Carrington, M.; Depledge, D.
361 P.; Fischer, S.; Gajria, B.; Gao, X.; Gardner, M. J.; Gingle, A.; Grant, G.; Harb, O. S.; Heiges, M.;
362 Hertz-Fowler, C.; Houston, R.; Innamorato, F.; Iodice, J.; Kissinger, J. C.; Kraemer, E.; Li, W.; Logan,
363 F. J.; Miller, J. A.; Mitra, S.; Myler, P. J.; Nayak, V.; Pennington, C.; Phan, I.; Pinney, D. F.;
364 Ramasamy, G.; Rogers, M. B.; Roos, D. S.; Ross, C.; Sivam, D.; Smith, D. F.; Srinivasamoorthy, G.;
365 Stoeckert, C. J. J.; Subramanian, S.; Thibodeau, R.; Tivey, A.; Treatman, C.; Velarde, G.; Wang, H.
366 TriTrypDB: A Functional Genomic Resource for the Trypanosomatidae. *Nucleic Acids Res* **2010**, *38*
367 (Database issue), D457-62. <https://doi.org/10.1093/nar/gkp851>.

368 (9) *TriTrypDB*. <https://tritrypdb.org/tritrypdb/app> (accessed 2023-06-13).

369 (10) Alonso, V. L.; Villanova, G. V.; Ritagliati, C.; Motta, M. C. M.; Cribb, P.; Serra, E. C. Trypanosoma
370 Cruzi Bromodomain Factor 3 Binds Acetylated α -Tubulin and Concentrates in the Flagellum
371 during Metacyclogenesis. *Eukaryot Cell* **2014**, *13* (6). <https://doi.org/10.1128/EC.00341-13>.

372 (11) Ritagliati, C.; Villanova, G. V.; Alonso, V. L.; Zuma, A. A.; Cribb, P.; Motta, M. C. M.; Serra, E. C.
373 Glycosomal Bromodomain Factor 1 from Trypanosoma Cruzi Enhances Trypomastigote Cell
374 Infection and Intracellular Amastigote Growth. *Biochemical Journal* **2016**, *473* (1).
375 <https://doi.org/10.1042/BJ20150986>.

376 (12) Villanova, G. V.; Nardelli, S. C.; Cribb, P.; Magdaleno, A.; Silber, A. M.; Motta, M. C.; Schenkman,
377 S.; Serra, E. Trypanosoma Cruzi Bromodomain Factor 2 (BDF2) Binds to Acetylated Histones and Is
378 Accumulated after UV Irradiation. *Int J Parasitol* **2009**, *39* (6), 665–673.
379 [https://doi.org/S0020-7519\(08\)00481-5 \[pii\] 10.1016/j.ijpara.2008.11.013](https://doi.org/S0020-7519(08)00481-5 [pii] 10.1016/j.ijpara.2008.11.013).

380 (13) Alonso, V. L.; Ritagliati, C.; Cribb, P.; Cricco, J. A.; Serra, E. C. Overexpression of Bromodomain
381 Factor 3 in Trypanosoma Cruzi (TcBDF3) Affects Differentiation of the Parasite and Protects It
382 against Bromodomain Inhibitors. *FEBS Journal* **2016**, *283* (11).
383 <https://doi.org/10.1111/febs.13719>.

384 (14) Pezza, A.; Tavernelli, L. E.; Alonso, V. L.; Perdomo, V.; Gabarro, R.; Prinjha, R.; Araya, E. R.; Rioja,
385 I.; Docampo, R.; Calderón, F.; Martin, J.; Serra, E. Essential Bromodomain TcBDF2 as a Drug Target
386 against Chagas Disease. *ACS Infect Dis* **2022**. <https://doi.org/10.1021/ACSINFCDIS.2C00057>.

387 (15) Rosón, J. N.; de Oliveira Vitarelli, M.; Costa-Silva, H. M.; Pereira, K. S.; da Silva Pires, D.; de Sousa
388 Lopes, L.; Cordeiro, B.; Kraus, A. J.; Cruz, K. N. T.; Calderano, S. G.; Fragoso, S. P.; Siegel, T. N.;
389 Elias, M. C.; da Cunha, J. P. C. Histone H2B.V Demarcates Strategic Regions in the Trypanosoma
390 Cruzi Genome, Associates with a Bromodomain Factor and Affects Parasite Differentiation and
391 Host Cell Invasion. *bioRxiv* **2021**.

392 (16) Trousdale, R. K.; Wolgemuth, D. J. Bromodomain Containing 2 (Brd2) Is Expressed in Distinct
393 Patterns during Ovarian Folliculogenesis Independent of FSH or GDF9 Action. *Mol Reprod Dev*
394 **2004**, *68* (3), 261–268. <https://doi.org/10.1002/mrd.20059>.

395 (17) Crowley, T. E.; Brunori, M.; Rhee, K.; Wang, X.; Wolgemuth, D. J. Change in Nuclear-Cytoplasmic
396 Localization of a Double-Bromodomain Protein during Proliferation and Differentiation of Mouse
397 Spinal Cord and Dorsal Root Ganglia. *Developmental Brain Research* **2004**, *149* (2), 93–101.
398 <https://doi.org/10.1016/j.devbrainres.2003.12.011>.

399 (18) Liu, H.; Li, X.; Niu, Z.; Zhang, L.; Zhou, M.; Huang, H.; He, J.; Zhang, W.; Xiao, L.; Tang, Y.; Wang, L.;
400 Li, G. Preparation of Polyclonal Antibody Specific for BRD7 and Detection of Its Expression Pattern
401 in the Human Fetus. *Journal of Histochemistry and Cytochemistry* **2008**, *56* (6), 531–538.
402 <https://doi.org/10.1369/jhc.7A7340.2007>.

403 (19) Denis, G. V. Bromodomain Motifs and “Scaffolding”? *Front Biosci* **2001**, *6*, D1065.
404 <https://doi.org/10.2741/A668>.

405 (20) Wang, Q.; Shao, X.; Leung, E. L. H.; Chen, Y.; Yao, X. Selectively Targeting Individual
406 Bromodomain: Drug Discovery and Molecular Mechanisms. *Pharmacol Res* **2021**, *172*, 105804.
407 <https://doi.org/10.1016/j.phrs.2021.105804>.

408 (21) Schulz, D.; Mugnier, M. R.; Paulsen, E. M.; Kim, H. S.; Chung, C. wa W.; Tough, D. F.; Rioja, I.;
409 Prinjha, R. K.; Papavasiliou, F. N.; Debler, E. W. Bromodomain Proteins Contribute to
410 Maintenance of Bloodstream Form Stage Identity in the African Trypanosome. *PLoS Biol* **2015**, *13*
411 (12). <https://doi.org/10.1371/JOURNAL.PBIO.1002316>.

412 (22) García, P.; Alonso, V. L.; Serra, E.; Escalante, A. M.; Furlan, R. L. E. Discovery of a Biologically
413 Active Bromodomain Inhibitor by Target-Directed Dynamic Combinatorial Chemistry. *ACS Med
414 Chem Lett* **2018**, *9* (10), 1002–1006. <https://doi.org/10.1021/acsmmedchemlett.8b00247>.

415 (23) Ramallo, I. A.; Alonso, V. L.; Rua, F.; Serra, E.; Furlan, R. L. E. A Bioactive Trypanosoma Cruzi
416 Bromodomain Inhibitor from Chemically Engineered Extracts. *ACS Comb Sci* **2018**, *20* (4), 220–
417 228. <https://doi.org/10.1021/acscombsci.7b00172>.

418 (24) Chua, M. J.; Robaa, D.; Skinner-Adams, T. S.; Sippl, W.; Andrews, K. T. Activity of Bromodomain
419 Protein Inhibitors/Binders against Asexual-Stage Plasmodium Falciparum Parasites. *Int J Parasitol
420 Drugs Drug Resist* **2018**, *8* (2), 189–193. <https://doi.org/10.1016/j.ijpddr.2018.03.001>.

421 (25) Jeffers, V.; Yang, C.; Huang, S.; Sullivan, W. J. Bromodomains in Protozoan Parasites: Evolution,
422 Function, and Opportunities for Drug Development. *Microbiol Mol Biol Rev* **2017**, *81* (1).
423 <https://doi.org/10.1128/MMBR.00047-16>.

424 (26) Hanquier, J.; Gimeno, T.; Jeffers, V.; Sullivan, W. J. Evaluating the GCN5b Bromodomain as a
425 Novel Therapeutic Target against the Parasite Toxoplasma Gondii. *Exp Parasitol* **2020**, *211*,
426 107868. <https://doi.org/10.1016/J.EXPPARA.2020.107868>.

427 (27) Russell, C. N.; Carter, J. L.; Borgia, J. M.; Bush, J.; Calderón, F.; Gabarró, R.; Conway, S. J.;
428 Mottram, J. C.; Wilkinson, A. J.; Jones, N. G. Bromodomain Factor 5 as a Target for
429 Antileishmanial Drug Discovery. *ACS Infect Dis* **2023**, *9* (11), 2340–2357.
430 https://doi.org/10.1021/ACSINFECDIS.3C00431/SUPPL_FILE/ID3C00431_SI_002.XLSX.

431 (28) Pezza, A.; Tavernelli, L. E.; Alonso, V. L.; Perdomo, V.; Gabarro, R.; Prinjha, R.; Rodríguez Araya, E.;
432 Rioja, I.; Docampo, R.; Calderón, F.; Martin, J.; Serra, E. Essential Bromodomain TcBDF2 as a Drug
433 Target against Chagas Disease. *ACS Infect Dis* **2022**. <https://doi.org/10.1021/acsinfecdis.2c00057>.

434 (29) García, P.; Alonso, V. L.; Serra, E.; Escalante, A. M.; Furlan, R. L. E. Discovery of a Biologically
435 Active Bromodomain Inhibitor by Target-Directed Dynamic Combinatorial Chemistry. *ACS Med
436 Chem Lett* **2018**, *9* (10). <https://doi.org/10.1021/acsmedchemlett.8b00247>.

437 (30) Aldeghi, M.; Ross, G. A.; Bodkin, M. J.; Essex, J. W.; Knapp, S.; Biggin, P. C. Large-Scale Analysis of
438 Water Stability in Bromodomain Binding Pockets with Grand Canonical Monte Carlo.
439 *Communications Chemistry* **2018** *1:1* **2018**, *1* (1), 1–12.
440 <https://doi.org/10.1038/s42004-018-0019-x>.

441 (31) Alonso, V. L.; Manarin, R.; Perdomo, V.; Gulin, E.; Serra, E.; Cribb, P. In Vitro Drug Screening
442 against All Life Cycle Stages of Trypanosoma Cruzi Using Parasites Expressing β -Galactosidase.
443 *Journal of Visualized Experiments* **2021**, No. 177. <https://doi.org/10.3791/63210>.

444 (32) Gulin, J. E. N.; Rocco, D. M.; Alonso, V.; Cribb, P.; Altcheh, J.; Garcia-Bournissen, F. Optimization
445 and Biological Validation of an in Vitro Assay Using the Transfected Dm28c/PLacZ Trypanosoma
446 Cruzi Strain. *Biol Methods Protoc* **2021**, *6* (1). <https://doi.org/10.1093/biomet/bpab004>.

447 (33) Buckner, F. S.; Verlinde, C. L.; La Flamme, A. C.; Van Voorhis, W. C. Efficient Technique for
448 Screening Drugs for Activity against Trypanosoma Cruzi Using Parasites Expressing
449 Beta-Galactosidase. *Antimicrob Agents Chemother* **1996**, *40* (11), 2592–2597.

450 (34) Hendrickson, O. D.; Taranova, N. A.; Zherdev, A. V.; Dzantiev, B. B.; Eremin, S. A. Fluorescence
451 Polarization-Based Bioassays: New Horizons. *Sensors (Switzerland)*. 2020.
452 <https://doi.org/10.3390/s20247132>.

453 (35) Hall, M. D.; Yasgar, A.; Peryea, T.; Braisted, J. C.; Jadhav, A.; Simeonov, A.; Coussens, N. P.
454 Fluorescence Polarization Assays in High-Throughput Screening and Drug Discovery: A Review.

455 *Methods and Applications in Fluorescence*. 2016.
456 <https://doi.org/10.1088/2050-6120/4/2/022001>.

457 (36) Bamborough, P.; Chung, C. W.; Furze, R. C.; Grandi, P.; Michon, A. M.; Sheppard, R. J.; Barnett, H.;
458 Diallo, H.; Dixon, D. P.; Douault, C.; Jones, E. J.; Karamshi, B.; Mitchell, D. J.; Prinjha, R. K.; Rau, C.;
459 Watson, R. J.; Werner, T.; Demont, E. H. Structure-Based Optimization of Naphthyridones into
460 Potent ATAD2 Bromodomain Inhibitors. *J Med Chem* **2015**, *58* (15), 6151–6178.
461 https://doi.org/10.1021/ACS.JMEDCHEM.5B00773/SUPPL_FILE/JM5B00773_SI_002.CSV.

462 (37) Humphreys, P. G.; Bamborough, P.; Chung, C. W.; Craggs, P. D.; Gordon, L.; Grandi, P.; Hayhow, T.
463 G.; Hussain, J.; Jones, K. L.; Lindon, M.; Michon, A. M.; Renaux, J. F.; Suckling, C. J.; Tough, D. F.;
464 Prinjha, R. K. Discovery of a Potent, Cell Penetrant, and Selective P300/CBP-Associated Factor
465 (PCAF)/General Control Nonderepressible 5 (GCN5) Bromodomain Chemical Probe. *J Med Chem*
466 **2017**, *60* (2), 695–709.
467 https://doi.org/10.1021/ACS.JMEDCHEM.6B01566/SUPPL_FILE/JM6B01566_SI_002.CSV.

468 (38) Demont, E. H.; Bamborough, P.; Chung, C. W.; Craggs, P. D.; Fallon, D.; Gordon, L. J.; Grandi, P.;
469 Hobbs, C. I.; Hussain, J.; Jones, E. J.; Le Gall, A.; Michon, A. M.; Mitchell, D. J.; Prinjha, R. K.;
470 Roberts, A. D.; Sheppard, R. J.; Watson, R. J. 1,3-Dimethyl Benzimidazolones Are Potent, Selective
471 Inhibitors of the Brpf1 Bromodomain. *ACS Med Chem Lett* **2014**, *5* (11), 1190–1195.
472 https://doi.org/10.1021/ML5002932/SUPPL_FILE/ML5002932_SI_001.PDF.

473 (39) Theodoulou, N. H.; Bamborough, P.; Bannister, A. J.; Becher, I.; Bit, R. A.; Che, K. H.; Chung, C. W.;
474 Dittmann, A.; Drewes, G.; Drewry, D. H.; Gordon, L.; Grandi, P.; Leveridge, M.; Lindon, M.;
475 Michon, A. M.; Molnar, J.; Robson, S. C.; Tomkinson, N. C. O.; Kouzarides, T.; Prinjha, R. K.;
476 Humphreys, P. G. Discovery of I-BRD9, a Selective Cell Active Chemical Probe for Bromodomain
477 Containing Protein 9 Inhibition. *J Med Chem* **2016**, *59* (4), 1425–1439.
478 https://doi.org/10.1021/ACS.JMEDCHEM.5B00256/SUPPL_FILE/JM5B00256_SI_001.PDF.

479 (40) Chen, P.; Chaikuad, A.; Bamborough, P.; Bantscheff, M.; Bountra, C.; Chung, C. W.; Fedorov, O.;
480 Grandi, P.; Jung, D.; Lesniak, R.; Lindon, M.; Müller, S.; Philpott, M.; Prinjha, R.; Rogers, C.;
481 Selenski, C.; Tallant, C.; Werner, T.; Willson, T. M.; Knapp, S.; Drewry, D. H. Discovery and
482 Characterization of GSK2801, a Selective Chemical Probe for the Bromodomains BAZ2A and
483 BAZ2B. *J Med Chem* **2016**, *59* (4), 1410–1424.
484 https://doi.org/10.1021/ACS.JMEDCHEM.5B00209/SUPPL_FILE/JM5B00209_SI_001.PDF.

485 (41) Zhang, J. H.; Chung, T. D. Y.; Oldenburg, K. R. A Simple Statistical Parameter for Use in Evaluation
486 and Validation of High Throughput Screening Assays. *SLAS Discovery* **1999**, *4* (2), 67–73.
487 <https://doi.org/10.1177/108705719900400206>.

488 (42) Hewings, D. S.; Rooney, T. P. C.; Jennings, L. E.; Hay, D. A.; Schofield, C. J.; Brennan, P. E.; Knapp,
489 S.; Conway, S. J. Progress in the Development and Application of Small Molecule Inhibitors of
490 Bromodomain-Acetyl-Lysine Interactions. *J Med Chem* **2012**, *55* (22), 9393–9413.
491 https://doi.org/10.1021/JM300915B/ASSET/IMAGES/MEDIUM/JM-2012-00915B_0027.GIF.

492 (43) Aldeghi, M.; Ross, G. A.; Bodkin, M. J.; Essex, J. W.; Knapp, S.; Biggin, P. C. Large-Scale Analysis of
493 Water Stability in Bromodomain Binding Pockets with Grand Canonical Monte Carlo.
494 *Communications Chemistry* 2018 1:1 **2018**, 1 (1), 1–12.
495 <https://doi.org/10.1038/s42004-018-0019-x>.

496 (44) Chung, C. W.; Dean, A. W.; Woolven, J. M.; Bamborough, P. Fragment-Based Discovery of
497 Bromodomain Inhibitors Part 1: Inhibitor Binding Modes and Implications for Lead Discovery. *J
498 Med Chem* 2012, 55 (2), 576–586.
499 https://doi.org/10.1021/JM201320W/SUPPL_FILE/JM201320W_SI_001.PDF.

500 (45) Zhang, M.; Zhang, Y.; Song, M.; Xue, X.; Wang, J.; Wang, C.; Zhang, C.; Li, C.; Xiang, Q.; Zou, L.;
501 Wu, X.; Wu, C.; Dong, B.; Xue, W.; Zhou, Y.; Chen, H.; Wu, D.; Ding, K.; Xu, Y. Structure-Based
502 Discovery and Optimization of Benzo [d] Isoxazole Derivatives as Potent and Selective BET
503 Inhibitors for Potential Treatment of Castration-Resistant Prostate Cancer (CRPC). *J Med Chem*
504 2018, 61 (7), 3037–3058.
505 https://doi.org/10.1021/ACS.JMEDCHEM.8B00103/SUPPL_FILE/JM8B00103_SI_003.CSV.

506 (46) De Rycker, M.; Thomas, J.; Riley, J.; Brough, S. J.; Miles, T. J.; Gray, D. W. Identification of
507 Trypanocidal Activity for Known Clinical Compounds Using a New Trypanosoma Cruzi
508 Hit-Discovery Screening Cascade. *PLoS Negl Trop Dis* 2016, 10 (4), e0004584.
509 <https://doi.org/10.1371/JOURNAL.PNTD.0004584>.

510 (47) Ashby, E.; Paddock, L.; Betts, H. L.; Liao, J.; Miller, G.; Porter, A.; Rollosen, L. M.; Saada, C.; Tang,
511 E.; Wade, S. J.; Hardin, J.; Schulz, D. Genomic Occupancy of the Bromodomain Protein Bdf3 Is
512 Dynamic during Differentiation of African Trypanosomes from Bloodstream to Procyclic Forms.
513 *mSphere* 2022. <https://doi.org/10.1128/msphere.00023-22>.

514 (48) Yang, X.; Wu, X.; Zhang, J.; Zhang, X.; Xu, C.; Liao, S.; Tu, X. Recognition of Hyperacetylated
515 N-Terminus of H2AZ by TbBDF2 from Trypanosoma Brucei. *Biochemical Journal* 2017, 474 (22),
516 3817–3830. <https://doi.org/10.1042/BCJ20170619>.

517 (49) Staneva, D. P.; Carloni, R.; Auchyannikava, T.; Tong, P.; Rappsilber, J.; Arockia Jeyaprakash, A.;
518 Matthews, K. R.; Allshire, R. C. A Systematic Analysis of Trypanosoma Brucei Chromatin Factors
519 Identifies Novel Protein Interaction Networks Associated with Sites of Transcription Initiation and
520 Termination. *Genome Res* 2021, 31 (11), 2138–2154.
521 <https://doi.org/10.1101/GR.275368.121/-/DC1>.

522 (50) Jones, N. G.; Geoghegan, V.; Moore, G.; Carnielli, J. B. T.; Newling, K.; Calderón, F.; Gabarró, R.;
523 Martín, J.; Prinjha, R. K.; Rioja, I.; Wilkinson, A. J.; Mottram, J. C. Bromodomain Factor 5 Is an
524 Essential Regulator of Transcription in Leishmania. *Nature Communications* 2022 13:1 **2022**, 13
525 (1), 1–18. <https://doi.org/10.1038/s41467-022-31742-1>.

526 (51) Ramallo, I. A.; Alonso, V. L.; Rua, F.; Serra, E.; Furlan, R. L. E. A Bioactive *Trypanosoma Cruzi*
527 Bromodomain Inhibitor from Chemically Engineered Extracts. *ACS Comb Sci* **2018**, *20* (4).
528 <https://doi.org/10.1021/acscombsci.7b00172>.

529